九州大学学術情報リポジトリ
Kyushu University Institutional Repository

A versatile method for surface functionalization and hydrophobization of gold nanoparticles

Ishida, Takuya
Department of Materials Physics and Chemistry, Graduate School of Engineering, Kyushu University

Yanaga, Yohei
Department of Materials Physics and Chemistry, Graduate School of Engineering, Kyushu University

Yamada, Sunao
Department of Applied Chemistry, Faculty of Engineering and Center for Future Chemistry, Kyushu University

Takahashi, Yukina
International Institute for Carbon Neutral Energy Research (I2CNER), Kyushu University

https://hdl.handle.net/2324/7174375

出版情報：Applied Surface Science. 546, pp.148932-, 2021-04-30. Elsevier
バージョン：
権利関係：

KYUSHU UNIVERSITY

A Versatile Method for Surface Functionalization and Hydrophobization of Gold Nanoparticles

Takuya Ishida[a,#], Yohei Yanaga[a], Sunao Yamada[b, ¶], Yukina Takahashi[c,d]*

[a] Department of Materials Physics and Chemistry, Graduate School of Engineering, Kyushu University, Fukuoka 819-0395, Japan.

[b] Department of Applied Chemistry, Faculty of Engineering and Center for Future Chemistry, Kyushu University, Fukuoka 819-0395, Japan

[c] International Institute for Carbon Neutral Energy Research (I2CNER), Kyushu University, Fukuoka 819- 0395, Japan

[d] JST, PRESTO, 4-1-8 Honcho, Kawaguchi, Saitama 332-0012, Japan

[#] Author Present Address: Institute of Industrial Science, the University of Tokyo, 4-6-1 Komaba, Meguro-ku, Tokyo 153-8505, Japan.

¶ Author Present Address: Institute of Systems, Information Technologies and Nanotechnologies, 2-1-22 Momochihama, Sawara-ku, Fukuoka 814-0001, Japan.

* Corresponding Author; Email: yukina@mail.cstm.kyushu-u.ac.jp

Highlights

- Large Au nanoparticles (AuNPs) were hydrophobidized and functionalized stably in a low-polar solvent.
- Thin films of the AuNPs were obtained by Langmuir–Blodgett method.
- The AuNPs showed surface-enhanced Raman scattering and enhanced photoluminescence.

ABSTRACT

A convenient, one-step, approach for surface modification with hydrophobic thiol or its dye-derivative of hydrophilic citrate-capped Au nanoparticles (Cit–AuNPs) is demonstrated. This method depended on the solubility of both Cit–AuNP and thiol or its derivative in the reaction solvent. We investigated a variety of solvents for Cit–AuNPs with 15–75 nm sizes and a capping molecule, octadecanethiol (ODT) or a disulfide derivative of hydrophobic porphyrin $(PC_{10}S)_2$. As to ODT,

surface immobilization of Cit–AuNPs with ODT was successful in 2-propanol, while *N*,*N*-dimethylformamide was best in the case of $(PC_{10}S)_2$. In both cases, surface modified AuNPs were redispersible even after storing under dried powder conditions. Two-dimensional monoparticle films of surface-modified AuNPs by the Langmuir–Blodgett method with ethylene glycol as subphase could be formed and exhibit surface-enhanced Raman scattering. Spectra from the porphyrin skeleton were certainly observed, with the maximum photoluminescence enhancement of 15-fold, around 50-nm size. As to AuNP with 17-nm diameter, mixed monolayer assemblies of $(PC_{10}S)_2$ and OT with different concentration ratios were fabricated and spectroscopic enhancement effects due to localized surface plasmon resonance were investigated.

Keywords

Localized surface plasmon resonance, Functionalized Au nanoparticle, Langmuir–Blodgett method, Surface-enhanced Raman scattering, Enhanced photoluminescence.

Graphical Abstract

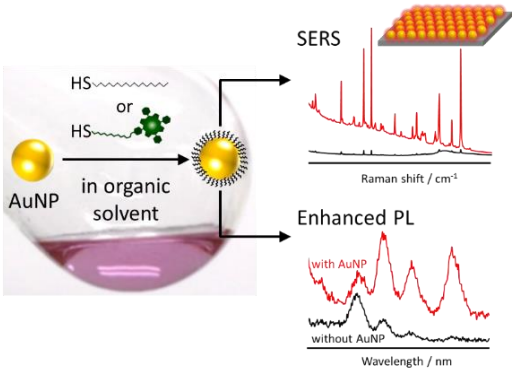

1. Introduction

Plasmonic nanoparticles have played a significant, central role on nanophotonics and nano-optics [1]. The strong interaction between the nanoparticle and light through localized surface plasmon resonance (LSPR)[2] has been utilized for surface-enhanced Raman scattering (SERS)[3,4] for improving efficiencies of light-emitting[5–7] and photoelectric conversion[8–12]. Physical and chemical properties of the nanoparticles (e.g., optical response, solubility, and stability), have been usually limited by a preparation method because types of chemical species adsorbed on the nanoparticle surface depend on the chemical reagents used in the preparation method. Therefore, modification of the nanoparticle surface with functional molecules has been studied extensively to control its physicochemical properties[4,6,7,13–27]. Even in the case of hydrophobization using alkanethiols[14,15,19,20,26] which is one of the simplest modification procedures (i.e., functionalization), it extends practical applications of the nanoparticles as photofunctional monoparticle films by using drop casting, spin coating, and Langmuir–Blodgett (LB) method[20,26]. Thus, the development of the preparation method of hydrophobic nanoparticles appropriate to purpose is basically important. For modification with the functional molecules including dyes, use of the organic solvent in which the nanoparticles are reacted with the molecules is unavoidable because most of the dyes usually dissolves only in the solvent. In the modification of nanoparticle surfaces with photofunctional molecules, a stepwise process of the preparation of organo-soluble nanoparticle at first, and then surface modification with functionalized molecules is usually employed[7,21–24]. However, in the organic solvent van der Waals interactions among nanoparticles, especially for larger sizes, often exceed electrostatic interaction and steric repulsion among the nanoparticles, so that it is hard to avoid irreversible aggregation (or agglomeration) of the particles [28–30]. For this reason, there have not yet been established methods to functionalize the particle in the organic solvent that is larger than ~50-nm exhibiting strong electric near-fields and thus suitable to study and apply enhanced photoluminescence (PL) events.

With respect to the issue of the surface modification of Au nanoparticles with 50-nm size, we have made three prerequisites in this study as follows: (i) hydrophobization, surface modification with dye molecules, and purification procedures (extraction and/or centrifugation) can be carried out as simple as possible, (ii) the size of the nanoparticle is sufficiently as large as ~50-nm exhibiting most strong near-field in the case of Au nanoparticle (AuNP)[31], and (iii) use of dispersion stabilizers such as surfactants and/or polymers is not used to prevent them as contaminants after purification process (e.g., centrifugation).

Previously, we reported that hydrophobic AuNPs with the size of ~50-nm could be prepared by mixing citrate-protected AuNP (Cit–AuNP) aqueous solution directly into ethanol (EtOH) solution of octadecanethiol (ODT)[26]. However, it was difficult to synthesize hydrophobic AuNPs with larger sizes of ~50-nm. Here, we carefully investigated organic solvents in which both the water-soluble

Cit–AuNPs and the organic-soluble functional molecules could be miscible, and developed a simple one-step procedure to surface-modify AuNPs with alkanethiol and/or a porphyrin dye with an alkyl-thiol tail (Scheme 1). We also carried out SERS and enhanced PL measurements of the above-described surface-modified AuNPs.

(a) Previous Report[26]

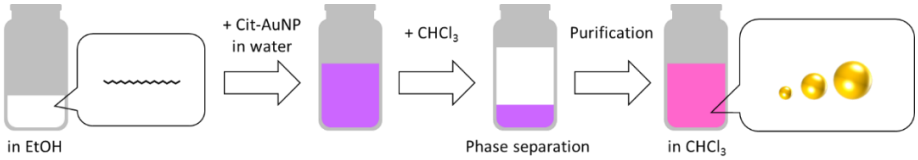

(b) This Study

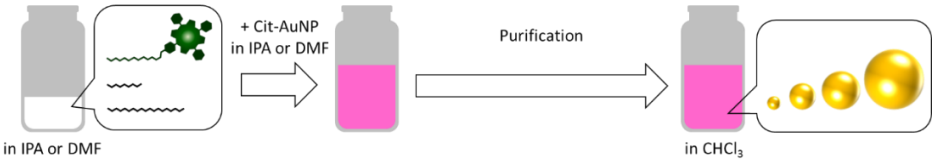

Scheme 1. Comparing the previous report[26] with a new method. Octanethiol (OT), Octadecanethiol (ODT), and $(PC_{10}S)_2$ (Figure S1) as a functional molecule were used.

2. Experimental

All starting materials were commercially purchased and used without further purification. Milli–Q water with the resistivity of 18.2 MΩ cm was used throughout the experiments. The synthesis of porphyrin-linked alkanethiol derivative $(PC_{10}S)_2$ (Figure S1) followed the literature we previously reported[8–12]. Synthetic scheme (Scheme S1) was shown in supporting information. UV–vis, photoluminescence, and Raman spectra were recorded on JASCO V-670ST, Horiba FluoroLog-R5509, Horiba LabRAM ARAMIS. Scanning electron microscopy (SEM) and transmission electron microscopy (TEM) were performed on Hitachi SU-8000 and JEOL JEM-200CX, respectively.

2.1. Cit–AuNP preparation

Citrate-capped AuNPs (Cit–AuNPs) were prepared by using citrate ion as a reducing reagent[32]. Namely, a solution of $HAuCl_4$ (0.010 wt% in Milli–Q water, 600 mL) was heated to the boiling temperature. Then, an aqueous solution of sodium citrate (1.0 wt%, 15.0, 7.38, 4.76, or 3.19 mL) was added to the boiling solution of $HAuCl_4$, giving Cit–AuNPs with the diameter of 17, 33, 48, or 75 nm, respectively. The reaction mixture was kept at the boiling temperature for 60 min, and was allowed to cool down to room temperature.

2.2. Test of solubility

The aqueous solution of as-prepared Cit–AuNP with the diameter of 48 nm (50 mL) was centrifuged (8 000 g, 15 min). The precipitate was redispersed in each solvent. The dispersion solvents were water; dimethyl sulfoxide (DMSO), *γ*-butyrolactone (GBL), *N,N*-dimethylformamide (DMF), acetonitrile, ethanol (EtOH), acetone, 2-propanol (IPA), dichloromethane (CH_2Cl_2), tetrahydrofuran (THF), chloroform ($CHCl_3$), and toluene. Furthermore, it was determined whether 2 mg of ODT and $(PC_{10}S)_2$ were soluble in 50 mL of these solvents. The criterion is defined as "visually smoothly soluble in the solvent", giving priority to convenience because the solubility test is a screening to reduce the risk of aggregation and irreversible precipitate of AuNPs in the modification reaction.

2.3. ODT–AuNP preparation

Hydrophobic AuNPs were prepared from Cit–AuNPs by a ligand-exchange process. The aqueous solution of prepared Cit–AuNP with each size (100 mL) was centrifuged (8 000 g for 17 and 33 nm, or 5 000 g for 48 and 75 nm, 15 min), and then the precipitate was redispersed in IPA (60 mL). Subsequently, an IPA solution of octadecanethiol (ODT) (1.0 mM, 6.0 mL) was added to the colloidal IPA solution (60 mL) under stirring for 3 days. After sonicating the reaction mixture for ~1 min, the solution was centrifuged (15 000 g, 15 min for 17 and 33 nm, or 12 000 g, 15 min for 48

and 75 nm). This operation was repeated 3 times so as to remove excess ODT, and the precipitate was redispersed to $CHCl_3$ (60 mL). When they was stored as a solid, the ODT–AuNPs were dried with an evaporator and then vacuum-dried for 3 h.

2.4. $PC_{10}S$–AuNP preparation

The aqueous solution of prepared Cit–AuNP with each size (400 mL) was centrifuged (8 000 g for 17 and 33 nm, or 5 000 g for 48 and 75 nm, 15 min), and then the precipitate was redispersed in DMF (40 mL). Subsequently, the colloidal solution was added to a mixed solution composed of a THF solution of $(PC_{10}S)_2$ (4 mg, 12 mL) diluted with DMF (188 mL) under stirring for 3 days. The solution was centrifuged (15 000 g, 15 min for 17 and 33 nm, or 12 000 g, 15 min for 48 and 75 nm), and then was redispersed to THF (200 mL). The solution was centrifuged again under the same conditions, redispersed in a mixed solvent of THF: DMF = 1: 1 (200 mL). The mixture solution was stirred for 6 h to remove physisorption of $(PC_{10}S)_2$. The solution was centrifuged (15 000 g for 17 and 33 nm, or 12 000 g for 48 and 75 nm, 15 min, 2 times), and then was redispersed to $CHCl_3$ including 3% DMF (200 mL). When they was stored as a solid, the $PC_{10}S$–AuNPs were dried with an evaporator and then vacuum-dried for 3 h. To evaluate the amount of $PC_{10}S$ adsorbed on the surface, the AuNPs were decomposed with an iodine solution, and the dissociated molecules were quantified by absorption measurement[21,23,24].

2.5. Control of adsorption degree of $PC_{10}S$

$(PC_{10}S)_2$ DMF solution (1.0 mM) was mixed with octanethiol (OT) DMF solution (1.0 mM) in any ratio. The mixed solution (50 mL), which included 0, 16.7, 26.9, or 40.9 mL of the OT solution ([OT]/[$(PC_{10}S)_2$] was 0, 0.5, 1.2, and 4.5) was stirred for 6 h. The Cit–AuNP DMF solution with the diameter of 17 nm (10 mL) was added to the OT–$(PC_{10}S)_2$ solution under stirring, and was reacted for 3 days. The solution was centrifuged (15 000 g, 15 min), and then was redispersed to THF (50 mL). The solution was centrifuged again under the same conditions, was redispersed in a mixed solvent of THF: DMF = 1: 1 (50 mL), and was stirred for 6 h. The solution was centrifuged (15 000 g, 15 min, 2 times), and then was redispersed to $CHCl_3$ including 3% DMF (50 mL).

2.6. Fabrication of AuNP thin-film

Monoparticle films composed of ODT–AuNP with the diameter of 17, 33, 48, or 75 nm on a smooth indium–tin oxide (ITO)-coated glass plate were fabricated by the Langmuir–Blodgett (LB) technique. First, dried ODT–AuNPs (1.0 mg for 17 and 33 nm, 1.5 mg for 48 and 75 nm) were redispersed into $CHCl_3$ (200 μL). Then, 200 μL solution of ODT–AuNP was spread on the surface of ethylene glycol as the subphase in the LB trough (USI-3-22QY, USI, Japan) at 25 °C, and kept for 15 min to evaporate the solvent. The resultant nanoparticle film was compressed at a speed of 0.1

mm s^{-1}, and then transferred onto an ITO substrate by Langmuir–Schaefer method at a speed of 0.1 mm s^{-1}. The monoparticle film on the ITO substrate was dried for 1 h and then slowly immersed in water to remove a little ethylene glycol remaining. Then, it was vacuum-dried for 3 h. The ITO substrate was beforehand cleaned by ultrasonication in water and EtOH for 5 min, followed by drying it with nitrogen gas. The substrate was immersed a mixed solution composed of H_2O_2 and NH_3 (H_2O_2: NH_3 = 1: 3) for 1 h at 50 °C, followed by immersion to 2% hexyltrimethoxysilane EtOH solution overnight. After washing by water and EtOH, the substrate was cleaned by ultrasonication. Furthermore, this substrate was heated on a hot plate at 80 ° C for 2 h.

3. Results and Discussion

3.1. Modification of AuNP with Molecules.

As mentioned in the introduction, it has been a considerable issue how large AuNP can be modified in organic solvents and stably dispersed, in terms of film fabrication with monoparticle layer levels using drop casting, spin coating, and LB method. In this respect, surface modification of AuNP with hydrophobic organic layers is basically important. Fortunately, both octadecanethiol (ODT) and porphyrin-linked alkanethiol derivative ($(PC_{10}S)_2$, Figure S1)[8–12] could be soluble in a varieties of organic solvents, as shown below. Thus, a key to overcome the above issue must be to find out appropriate organic solvents in which all AuNP (Cit–AuNP), ODT, and $(PC_{10}S)_2$ are also soluble without agglomeration. Here, we investigated several organic solvents in which citrate-capped AuNP (Cit–AuNP), ODT, and $(PC_{10}S)_2$ for modification were soluble, in order to select the appropriate solvent to realize one-step surface-modification procedure. First, Cit–AuNP aqueous solutions of each particle size (17, 33, 48, 75 nm) were prepared by the citrate-reduction method, and after centrifugation, an organic solvent to be capable of redispersing the resultant precipitate (Table 1). As a result, Cit–AuNP was redispersed into water, *γ*-butyrolactone (GBL), *N*,*N*-dimethylformamide (DMF), and 2-propanol (IPA), maintaining a stable isolated dispersion state (Figure S2). Also, it was redispersed into dimethyl sulfoxide (DMSO), appearing no precipitation, but the color of the solution changed to purple probably due to some aggregation. The other organic solvents were found to cause neither redispersion nor precipitation. In the range we investigated so far, the Cit–AuNP could be redispersed in the organic solvents with the dielectric constant of higher than ~18 and the molecular weight of higher that ~60, except water. From this result, it implies that the solvent molecule requires a certain degree of polarity and bulkiness to enable redispersion of the Cit–AuNP stably.

Next, we investigated the solvents in which ODT and $(PC_{10}S)_2$ were miscible (Table 1). The solvents which could dissolve both Cit–AuNP the thiol molecules were IPA and DMF in the case of ODT, while DMF and GBL in the case of $(PC_{10}S)_2$. Therefore, in the case of surface modification with ODT or $(PC_{10}S)_2$, IPA or DMF were used, respectively.

Table 1. Solubility of Cit–AuNP, ODT, and $(PC_{10}S)_2$. Water (H_2O), dimethyl sulfoxide (DMSO), *γ*-butyrolactone (GBL), *N,N*-dimethylformamide (DMF), acetonitorile (ACN), ethanol (EtOH), acetone (ACON), 2-propanol (IPA), dichloromethane (CH_2Cl_2), tetrahydrofuran (THF), and chloroform ($CHCl_3$) were used as solvents. MW stands for molecular weight. S, SN, SC, and I mean soluble, soluble and no change of solution color, soluble and change of solution color, and insoluble, respectively (S for ODT and $(PC_{10}S)_2$, SN and SC for Cit-AuNP).

	Redispersed Cit-AuNP[a]	ODT[b]	$(PC_{10}S)_2$[b]	Relative Permittivity	MW
H_2O	SN	I	I	80	18

DMSO	SC	I	I	47	78
GBL	SN	I	S	39	86
DMF	SN	S	S	38	73
ACN	I	I	I	37	41
EtOH	I	S	I	24	46
ACON	I	S	I	21	58
IPA	SN	S	I	18	60
CH_2Cl_2	I	S	S	9.1	85
THF	I	S	S	7.5	72
$CHCl_3$	I	S	S	4.8	119
Toluene	I		I	2.4	92

[a] SN, SC, and I stand for soluble and no change of solution color, soluble and change of solution color, and insoluble, respectively. [b] S and I mean soluble and insoluble, respectively.

In general, both thiol and disulfide derivatives chemisorb to AuNP through Au–S bond[33–37]. The AuNPs modified with ODT or $(PC_{10}S)_2$ were repeatedly centrifuged and redispersed into $CHCl_3$ (Figure S3). Figure 1 shows extinction spectra of Cit–AuNP aqueous solution, ODT–AuNP $CHCl_3$ solution, and $PC_{10}S$–AuNP $CHCl_3$ solution. Each absorption peak based on LSPR[2] was clearly observed in the range from 510 nm to 580 nm in all cases. As compared with Cit–AuNP in water, the plasmon peak of the modified AuNPs showed red-shift because refractive index around their surface increased owing to these adsorbed molecules and in the organic solvent.[38,39] Previously, we reported that the ODT–AuNPs with the size range from 17 to 48 nm were prepared in water–EtOH (50%v/v) mixed solvent[26]. In the present case, we succeeded in hydrophobizing AuNP with the size of 75 nm, though it was not successful in the previous method. These spectra in the case of 48 and 75 nm diameter were broadened owing to some aggregation with plasmon coupling as the size increased. In the extinction spectrum of $PC_{10}S$–AuNP, a broad Soret band of the porphyrin was observed around 420 nm[40–42]. Such broadening is due to aggregation of the porphyrins, suggesting that a densely-packed molecular layer is formed on the AuNP surface[41,42]. Furthermore, these AuNPs were vacuum-dried overnight and then redispersed into $CHCl_3$. Figure 2 shows the extinction spectra of redispersed ODT–AuNP and $PC_{10}S$–AuNP with the size of 17 nm after drying, followed by redispersion in $CHCl_3$ (Figure S4 for the other sizes). The shape of the extinction spectra hardly changed even after redispersion. In addition, the AuNPs could be redispersed into the solvent even after one month of dry storage under normal temperature and atmospheric conditions. Accordingly, it was demonstrated that the dried solid-state of the modified AuNPs can be redispersible in the non-polar solvent. In other words, the obtained ODT–AuNP and $PC_{10}S$–AuNP can be stored as the solid state under normal temperature and atmospheric conditions. It is significant to be solid except when using the AuNPs because, in general, the alkanethiol molecules adsorbed on the Au surface through the Au–S bond gradually desorb into solution or into vacuum[43–45]. The yield of the modified AuNPs was in the range of 20–60% for all size in terms of weight ratio of Au contained in the AuNP to that contained in $HAuCl_4$ aqueous solution. In the case of the AuNPs with the diameter of 17 nm, which has the largest specific surface area in this study, it is estimated that the density of ODT molecule on the AuNP surface is ~8 nm^{-2} or less[46,47]. While, the density of $PC_{10}S$ molecule was ~0.7 nm^{-2} as determined from the iodine method (in Experimental 2.4)[21,23,24]. The results show that above 94 weight% of the AuNP was Au. Improving the yields and reducing variability are future issues.

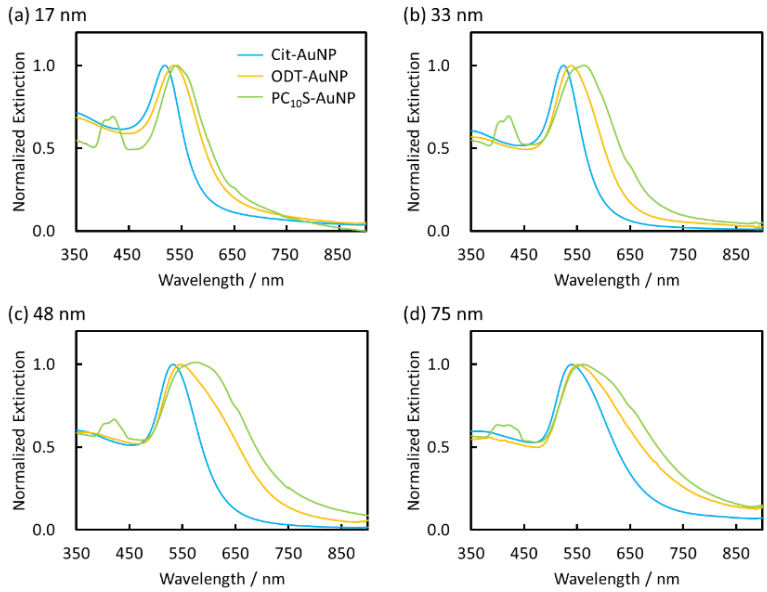

Figure 1. Extinction spectra of Cit–AuNP aqueous solution, ODT–AuNP $CHCl_3$ solution, and $PC_{10}S$–AuNP $CHCl_3$ solution with diameter of (a) 17, (b) 33, (c) 48, and (d) 75 nm.

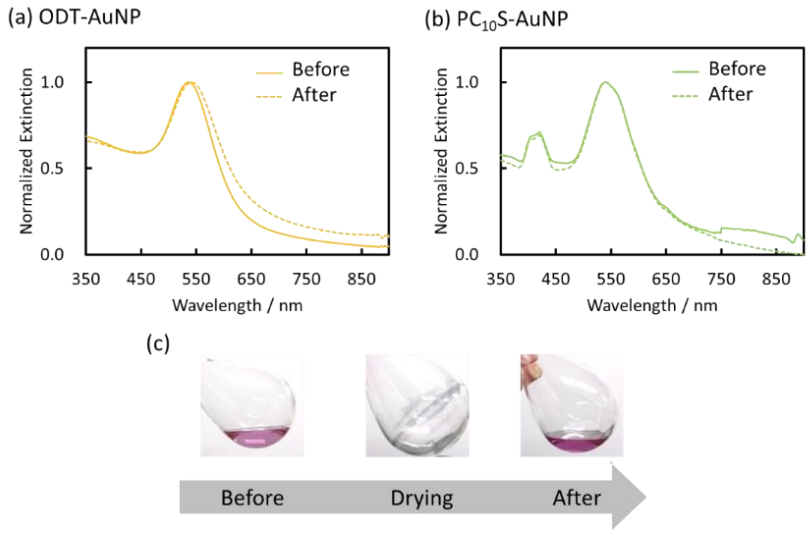

Figure 2. Extinction spectra of (a) ODT–AuNP and (b) $PC_{10}S$–AuNP with the diameter of 17 nm in $CHCl_3$ before and after vacuum-drying. (c) Photographs of ODT–AuNPs $CHCl_3$ solution before drying (left), after vacuum evaporation and (b) subsequent redispersion into $CHCl_3$.

The adsorption degree of the $PC_{10}S$ molecules on the AuNP surface can also be changed by using different concentration ratios of $(PC_{10}S)_2$ to alkanethiol. In order to suppress the formation of porphyrin aggregates, octanethiol (OT) which has the same length as the alkyl chain part of $PC_{10}S$ was added, and the concentration ratio of $(PC_{10}S)_2$ to OT was changed as the concentration ratio

([OT]/[$(PC_{10}S)_2$]) was 0, 0.5, 1.2, and 4.5, respectively in DMF, in which all species of Cit–AuNP with the size of 17 nm, $(PC_{10}S)_2$, and OT were soluble. Figure 3 shows the extinction spectra of surface-modified AuNP in $CHCl_3$, after above treatment processes. As the concentration ratio decreased, the Soret band of $PC_{10}S$ as a monomer at ~420 nm increased[40–42], and then it tended to decrease and another absorption originating from H-aggregates at ~400 nm concomitantly increased gradually[41,42]. These results show that the adsorption amount of $PC_{10}S$ molecule and the adsorption state could be controlled through change in the concentration ratio in the reaction solution. Furthermore, although place exchange reaction, which is a two-step molecular modification method, has been reported so far[48,49], our method demonstrates that the AuNP with a certain size exhibiting clearly LSPR can be modified with one- or two-types of molecules by one-step.

In order to demonstrate the usefulness of functionalized AuNPs, we investigated SERS spectra of dense ODT–AuNP films and photoluminescence enhancement of $PC_{10}S$–AuNP solution.

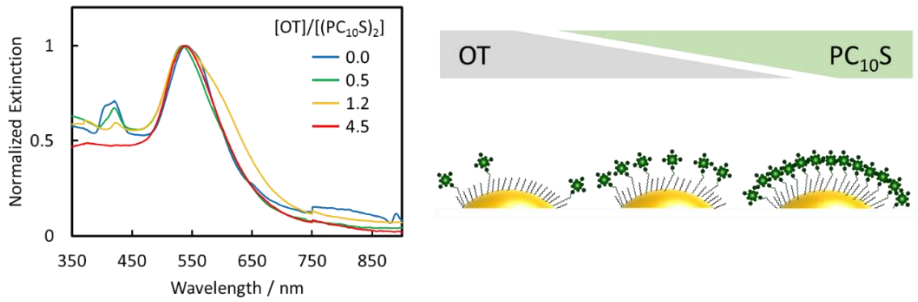

Figure 3. Extinction spectra of AuNP modified with OT and $PC_{10}S$ in $CHCl_3$ solution. The concentration ratio of OT to $(PC_{10}S)_2$ ([OT]/[$(PC_{10}S)_2$]) was 0.0, 0.5, 1.2, and 4.5 in the reaction solution.

3.2. SERS of ODT–AuNP film.

Our group and other groups have used bottom-up methods to fabricate array structures, such as electrodeposition[50,51], electrostatic layer-by-layer adsorption[52–55], electrophoretic approach[56], liquid-liquid interface[55,57–59], and LB techniques[20,26]. In particular, the LB method is an excellent technique for the preparation of monoparticle film of AuNP film with a high density and, especially a large area[20,26]. Actually, the LB monoparticle film of ODT–AuNPs could be formed and was transferred onto an ITO substrate. Previously, we prepared the LB film of AuNP by utilizing polyethylene glycol (PEG) as an amphiphilic agent added to water subphase[26]. PEG assists spreading of the hydrophobic AuNPs on water and to form the uniform monoparticle layer. In the measurements of SERS of the LB ODT–AuNP film, however, PEG should be removed from the LB film in order to avoid unwanted signals from PEG, inspite that the removing process was rather troublesome. Preparation of thiolated PEG-immobilized AuNPs is one of the excellent methods for hydrophobizing AuNPs in an aqueous solution, but it is not suitable for application such as vibrational

spectroscopy. In this study, ethylene glycol (EG) was employed as the subphase instead of water, to uniformly spread the AuNPs without PEG[60]. In fact, EG could be easily removed only by immersing the LB AuNP film on the ITO substrate into water. Figure 4a–d show SEM images of LB ODT–AuNP films with the diameter of 17, 33, 48, and 75 nm ($PC_{10}S$–AuNP films in SI, Figure S5), respectively. It is found that monoparticle films with high density were formed. In the extinction spectra (Figure 4e), the peak wavelength of each film was red-shifted from 590 to 700 nm as the size increased, in longer wavelength region than that of the solution. This result shows that plasmon coupling between AuNPs becomes stronger with increasing in the particle size[61]. The plasmon band of the film composed of larger AuNPs was broader, which may be due to some aggregation in the solution (Figure 1)[62]. Then the $CHCl_3$ solution of phthalocyanine (CuPc) was spin-coated on the LB films of AuNPs with 17 and 48 nm, and Raman spectra were measured by Raman spectroscopy (Figure 4f and Figure S6). In the spectra, signals assigned to CuPc were clearly observed[63], and the intensity of the LB film sample was higher than that without the LB film, indicating the signal of SERS. The enhancement factor (EF) is defined as the value of dividing the scattering intensity with the AuNP film to that without the film. The EFs at 1530 cm^{-1} assigned to the symmetric stretching motion of isoindole groups were 7 and 31, respectively, and the LB film with 48 nm showed stronger enhancement. It is considered that the EF of the LB film with 48 nm is due to the overlapping of the laser wavelength (785 nm) with the broad extinction band, and thus the near electric field appreciably enhanced by plasmon coupling between the larger AuNPs.

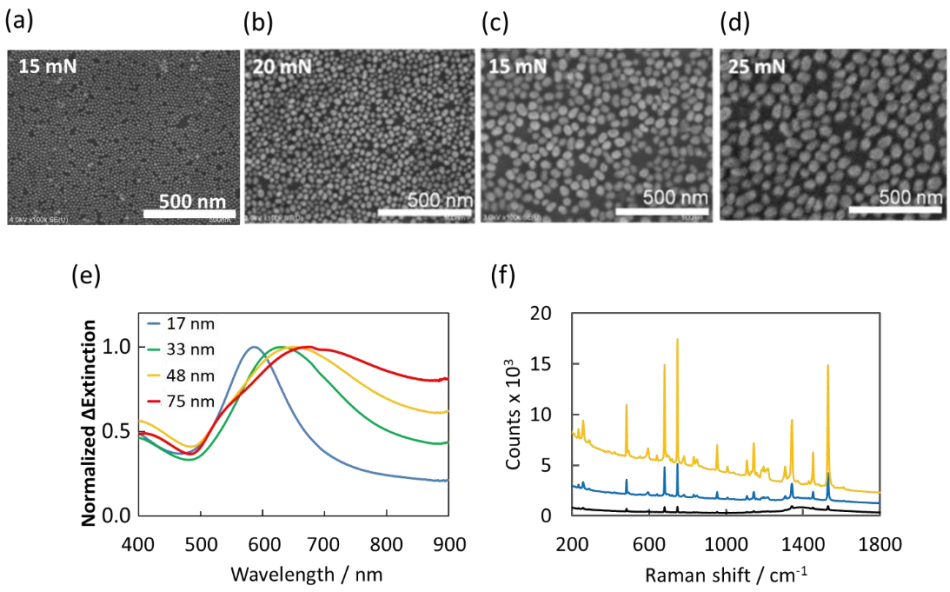

Figure 4. SEM images of ODT–AuNP LB film with the diameter of (a) 17, (b) 33, (c) 48, and (d) 75 nm. Surface pressure was shown in (a)–(d). (e) Extinction spectra of the LB films. (f) Raman spectra (laser wavelength = 785 nm) with ODT–AuNP LB films (diameter of 17 nm, blue: 48 nm, yellow) and without the film (black).

3.3. PL enhancement of AuNP colloidal solution.

Photoluminescence (PL) spectra of the $PC_{10}S$–AuNP $CHCl_3$ solution of each particle size were measured (Figure 5a and Figure S7). Excitation spectra were normalized by the amount of adsorption of $PC_{10}S$ molecules. As a result, an emission intensity at 720 nm increased with increasing in the particle size. It was largest in the 48 nm diameter. Figure 5b shows dependence of EFs at each excitation wavelength on the size. EF of photoluminescence is defined as the value obtained by dividing the intensity of $PC_{10}S$–AuNP with that of free $PC_{10}S$ in the solution. The EF of $PC_{10}S$–AuNP with 48 nm was 15 at 648 nm of the excitation wavelength. It is considered that the plasmon electric field amplified the excitation of $PC_{10}S$ because the enhancement was observed in the Q band (518–648 nm) whereas it was not observed in Soret band (420 nm). The size dependence of EF shows the same tendency as the strength of enhanced near field strength by LSPR[31].

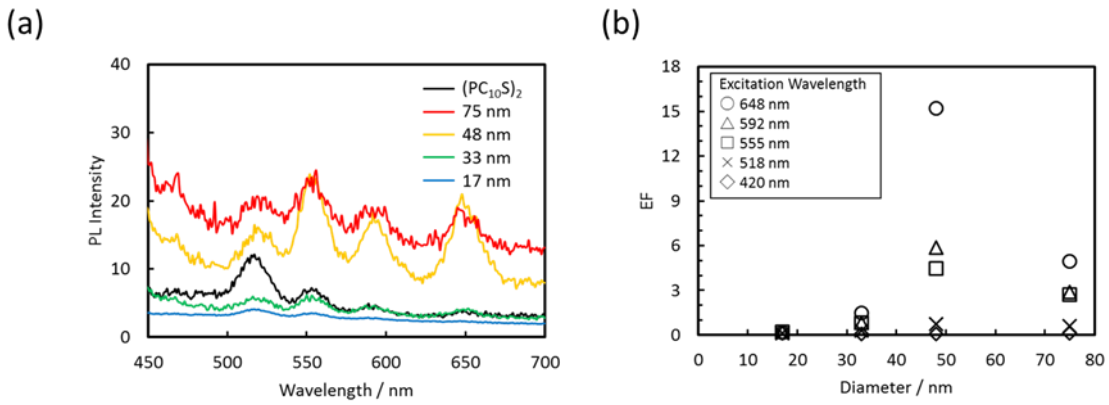

(a) Excitation spectra of photoluminescence (emission wavelength λ_{em} = 720 nm) and (b) Enhancement factor (EF) of emission. EF of photoluminescence is defined as the value obtained by dividing the intensity of $PC_{10}S$ with AuNP by that of free $PC_{10}S$ in the solution.

4. Conclusions

An one-step surface modification of AuNPs with three types of hydrophobic molecules in organic solvents was developed. The results were ascribed from solubilities of both citrate-capped AuNP and the molecules for surface modification, without causing aggregation. The result also made possible the change of the concentration ratio of the mixed molecular assembly on AuNP. Furthermore, it made possible easier fabrication of the PEG-free LB films of surface-modified AuNP with monolayer, enabling clear SERS, and improved the photoluminescence of the $PC_{10}S$–AuNP colloid solution. This preparation approach will substantially contribute to the development of plasmonic researches as well as its practical applications to photonic devices.

Acknowledgements

This work was supported by a Grant-in-Aid for Young Scientists (A) (for YT JP16H06120) from JSPS, PRESTO (for YT JPMJPR1908) from JST, and the research grant of Asahi Glass Foundation (for YT).

5. References

[1] J. A. Schuller, E. S. Barnard, W. Cai, Y. C. Jun, J. S. White, M. L. Brongersma, Plasmonics for extreme light concentration and manipulation, Nat. Mater. 9 (2010), 193–204.

[2] K. L. Kelly, E. Coronado, L. L. Zhao, G. C. Schatz, The optical properties of metal nanoparticles: The influence of size, shape, and dielectric environment, J. Phys. Chem. B 107 (2003), 668–677.

[3] D. L. Jeanmaire, R. P. Van Duyne, Surface raman spectroelectrochemistry: Part I. Heterocyclic, aromatic, and aliphatic amines adsorbed on the anodized silver electrode, J. Electroanal. Chem. 84 (1977), 1–20.

[4] A. B. S.-Montes, D. Jimenez de Aberasturi, J. Langer, J. J. G.-Casares, L. Scarabelli, A. Herrero, L. M. L.-Marzán, A general method for solvent exchange of plasmonic nanoparticles and self-assembly into SERS-active monolayers, Langmuir 31 (2015), 9205–9213.

[5] P. Anger, P. Bharadwaj, L. Novotny, Enhancement and quenching of single-molecule fluorescence, Phys. Rev. Lett. 96 (2006), 113002.

[6] J. Zhang, Y. Fu, M. H. Chowdhury, J. R. Lakowicz, Single-molecule studies on fluorescently labeled silver particles: effects of particle size, J. Phys. Chem. C 112 (2008), 18–26.

[7] Y. Kim, B. Kang, H.-Y. Ahn, J. Seo, K. T. Nam, Plasmon enhanced fluorescence based on porphyrin–peptoid hybridized gold nanoparticle platform, Small 13 (2017), 1700071.

[8] T. Akiyama, M. Nakada, N. Terasaki and S. Yamada, Photocurrent enhancement in a porphyrin-gold nanoparticle nanostructure assisted by localized plasmon excitation, Chem. Commun. (2006), 395–397.

[9] T. Akiyama, K. Aiba, K. Hoashi, M. Wang, K. Sugawa and S. Yamada, Enormous enhancement in photocurrent generation using electrochemically fabricated gold nanostructures, Chem. Commun. 46 (2010), 306–308.

[10] H. A. Atwater, A. Polman, Plasmonics for improved photovoltaic devices, Nat. Mater. 9 (2010), 205–213.

[11] K. Sugawa, S. Hirono, T. Akiyama, S. Yamada, Photocurrent enhancement tuned with plasmonic resonance in self-assembled monolayers fabricated on regularly arrayed gold nanostructures, Photochem. Photobiol. Sci. 11 (2012), 318–322.

[12] K. Sugawa, K. Uchida, N. Takeshima, S. Jin, N. Tsunenari, H. Takeda, Y. Kida, T. Akiyama, J. Otsuki, K. Takase, S. Yamada, Extraordinary enhancement of porphyrin photocurrent utilizing plasmonic silver arrays, Nanoscale 8 (2016), 15467–15472.

[13] H. Hirai, H. Aizawa, Preparation of stable dispersions of colloidal gold in hexanes by phase transfer, J. Colloid Interface Sci. 161(1993), 471–474.

[14] M. Giersig, P. Mulvaney, Preparation of ordered colloid monolayers by electrophoretic deposition, Langmuir 9 (1993), 3408–3413.

[15] M. Brust, M. Walker, D. Bethell, D. J. Schiffrin, R. Whyman, Synthesis of thiol-derivatised gold nanoparticles in a two-phase liquid–liquid system, J. Chem. Soc., Chem. Commun. 0 (1994), 801–802.

[16] R. Balasubramanian, B. Kim, S. L. Tripp, X. Wang, M. Lieberman, A. Wei, Dispersion and stability studies of resorcinarene-encapsulated gold nanoparticles, Langmuir 18 (2002), 3676–3681.

[17] J. M. McMahon, S. R. Emory, Phase transfer of large gold nanoparticles to organic solvents with increased stability, Langmuir 23 (2007), 1414–1418.

[18] X. Wang, S. Xu, J. Zhou, W. Xu, A rapid phase transfer method for nanoparticles using alkylamine stabilizers, J. Colloid Interface Sci. 348 (2010), 24–28.

[19] H. J. Baika, S. Hong, S. Park, Surface plasmon modes of gold nanospheres, nanorods, and nanoplates in an organic solvent: Phase-transfer from aqueous to organic media, J. Colloid Interface Sci. 358 (2011), 317–322.

[20] M. Toma, K. Toma, K. Michioka, Y. Ikezoe, D. Obara, K. Okamoto, K. Tamada, Collective plasmon modes excited on a silver nanoparticle 2D crystalline sheet, Phys. Chem. Chem. Phys. 13 (2011), 7459–7466.

[21] Y. Li, D. Yu, L. Dai, A. Urbas, Q. Li, Organo-soluble chiral thiol-monolayer-protected gold nanorods, Langmuir 27 (2011), 98–103.

[22] C. Xue, Y. Xu, Y. Pang, D. Yu, L. Dai, M. Gao, A. Urbas, Q. Li, Organo-soluble porphyrin mixed monolayer-protected gold nanorods with intercalated fullerenes, Langmuir 28 (2012), 5956–5963.

[23] C. Xue, O. Birel, M. Gao, S. Zhang, L. Dai, A. Urbas, Q. Li, Perylene monolayer protected gold nanorods: Unique optical, electronic properties and self-assemblies, J. Phys. Chem. C 116 (2012), 10396–10404.

[24] C. Xue, O. Birela, Y. Li, X. Ma, M. Gao, A. Urbas, Q. Li, Porphyrin metal complex monolayer-protected gold nanorods: A parallel facile synthesis and self-assembly, J. Colloid Interface Sci. 398 (2013), 1–6.

[25] L. A. Wijenayaka, M. R. Ivanov, C. M. Cheatum, A. J. Haes, Improved parametrization for extended derjaguin, landau, verwey, and overbeek predictions of functionalized gold nanosphere stability, J. Phys. Chem. C 119 (2015), 10064–10075.

[26] T. Ishida, Y. Tachikiri, T. Sako, Y. Takahashi, S. Yamada, Structural characterization and plasmonic properties of two-dimensional arrays of hydrophobic large gold nanoparticles fabricated by Langmuir–Blodgett technique, Appl. Surf. Sci. 404 (2017), 350–356.

[27] J. Zong, S. L. Cobb, N. R. Cameron, Peptide-functionalized gold nanoparticles: versatile biomaterials for diagnostic and therapeutic applications, Biomater. Sci. 5 (2017), 872–886.

[28] S. K. Sainis, J. W. Merrill, E. R. Dufresne, Electrostatic interactions of colloidal particles at

vanishing ionic strength, Langmuir 24 (2008), 13334–13337.
[29] Y. Yang, H. Qin, M. Jiang, L. Lin, T. Fu, X. Dai, Z. Zhang, Y. Niu, H. Cao, Y. Jin, F. Zhao, X. Peng, Entropic ligands for nanocrystals: from unexpected solution properties to outstanding processability, Nano Lett. 16 (2016), 2133–2138.
[30] H. T. Phan, A. J. Haes, What does nanoparticle stability mean?, J. Phys. Chem. C 123 (2019), 16495–16507.
[31] C. Deeb, X. Zhou, J. Plain, G. P. Wiederrecht, R. Bachelot, M. Russell, P. K. Jain, Size dependence of the plasmonic near-field measured via single-nanoparticle photoimaging, J. Phys. Chem. C 117 (2013), 10669–10676.
[32] J. Turkevich, Colloidal gold. Part II, Gold Bull. 18 (1985), 86–91.
[33] C. D. Bain, H. A. Biebuyck, G. M. Whitesides, Comparison of self-assembled monolayers on gold: coadsorption of thiols and disulfides, Langmuir 5 (1989), 723–727.
[34] L. H. Dubois, R. G. Nuzzo, Synthesis, structure, and properties of model organic surfaces, Annu. Rev. Phys. Chem. 43 (1992), 437–463.
[35] H. A. Biebuyck, C. D. Bain, G. M. Whitesides, Comparison of organic monolayers on polycrystalline gold spontaneously assembled from solutions containing dialkyl disulfides or alkanethiols, Langmuir 10 (1994), 1825–1831.
[36] R. G. Nuzzo, L. H. Dubois, D. L. Allara, Fundamental studies of microscopic wetting on organic surfaces. 1. Formation and structural characterization of a self-consistent series of polyfunctional organic monolayers, J. Am. Chem. Soc. 112 (1990), 558−569.
[37] T. P. Gustafson, Q. Cao, S. T. Wang, M. Y. Berezin, Design of irreversible optical nanothermometers for thermal ablations, Chem. Commun. 49 (2013), 680−682.
[38] S. Underwood, P. Mulvaney, Effect of the solution refractive index on the color of gold colloids, Langmuir 10 (1994), 3427–3430.
[39] K. M. Mayer, J. H. Hafner, Localized surface plasmon resonance sensors, Chem. Rev. 111 (2011), 3828–3857.
[40] M. Gouterman, Spectra of porphyrins, J. Mol. Spectrosc. 6 (1961), 6, 138–163.
[41] N. C. Maiti, S. Mazumdar, N. Periasamy, J- and H-aggregates of porphyrin−surfactant complexes: time-resolved fluorescence and other spectroscopic studies, J. Phys. Chem. B 102 (1998), 1528–1538.
[42] R. F. Khairutdinov, N. Serpone, Photoluminescence and transient spectroscopy of free base porphyrin aggregates, J. Phys. Chem. B 103 (1999), 761–769.
[43] C. D. Bain, E. B. Troughton, Y. T. Tao, J. Evall, G. M. Whitesides, R. G. Nuzzo, Formation of monolayer films by the spontaneous assembly of organic thiols from solution onto gold, J. Am. Chem. Soc. 111 (1989), 321–335.
[44] E. Ito, H. Kang, D. Lee, J. B. Park, M. Hara, J. Noh, Spontaneous desorption and phase

transitions of self-assembled alkanethiol and alicyclic thiol monolayers chemisorbed on Au(1 1 1) in ultrahigh vacuum at room temperature, J. Colloid Interface Sci. 394 (2013), 522–529.

[45] M. Borzenkov, G. Chirico, L. D'Alfonso, L. Sironi, M. Collini, E. Cabrini, G. Dacarro, C. Milanese, P. Pallavicini, A. Taglietti, C. Bernhard, F. Denat, Thermal and chemical stability of thiol bonding on gold nanostars, Langmuir 31 (2015), 8081–8091.

[46] S. Elzey, D.-H. Tsai, S. A. Rabb, L. L. Yu, M. R. Winchester, V. A. Hackley, Quantification of ligand packing density on gold nanoparticles using ICP-OES, Anal. Bioanal. Chem. 403 (2012), 145–149.

[47] H. Hinterwirth, S. Kappel, T. Waitz, T. Prohaska, W. Lindner, M. Lämmerhofer, Quantifying thiol ligand density of self-assembled monolayers on gold nanoparticles by inductively coupled plasma–mass spectrometry, ACS Nano 7 (2013), 1129–1136.

[48] M. J. Hostetler, A. C. Templeton, R. W. Murray, Dynamics of place-exchange reactions on monolayer-protected gold cluster molecules, Langmuir 15 (1999), 3782–3789.

[49] Y. Song, R. W. Murray, Dynamics and extent of ligand exchange depend on electronic charge of metal nanoparticles, J. Am. Chem. Soc. 124 (2002), 7096–7102.

[50] Y. Takahashi, T. Tatsuma, Electrodeposition of thermally stable gold and silver nanoparticle ensembles through a thin Al_2O_3 nanomask , Nanoscale, 2 (2010), 1494–1499.

[51] T. Ishida, M. Katagishi, Y. Takahashi, S. Yamada, Space optimization for utilization of plasmonic effect on a P3HT-gold nanoparticle photoelectrode, Chem. Lett. 46 (2017), 1612–1615.

[52] J. Schmitt, G. Decher, W. J. Dressick, S. L. Brandow, R. E. Geer, R. Shashidhar, J. M. Calvert, Metal nanoparticle/polymer superlattice films: Fabrication and control of layer structure, Adv. Mater. 9 (1997), 61–65.

[53] T. Yonezawa, S. Onoue, T. Kunitake, Growth of closely packed layers of gold nanoparticles on an aligned ammonium surface, Adv. Mater. 10 (1998), 414–416.

[54] T. Arakawa, T. Munaoka, T. Akiyama, S. Yamada, Effects of silver nanoparticles on photoelectrochemical responses of organic dyes, J. Phys. Chem. C 113 (2009), 11830–11835.

[55] Y. Takahashi, S. Taura, T. Akiyama, S. Yamada, Electropolymerized polythiophene photoelectrodes with density-controlled gold nanoparticles, Langmuir 28 (2012), 9155–9160.

[56] N. Chandrasekharan, P. V. Kamat, Assembling gold nanoparticles as nanostructured films using an electrophoretic approach, Nano Lett. 1 (2001), 67–70.

[57] M. Suzuki, Y. Niidome, N. Terasaki, K. Inoue, Y. Kuwahara, S. Yamada, Surface-enhanced nonresonance Raman scattering of rhodamine 6G molecules adsorbed on gold nanorod films, Jpn. J. Appl. Phys., 43 (2004), L554.

[58] F. Reincke, S. G. Hickey, W. K. Kegel, D. Vanmaekelbergh, Spontaneous assembly of a monolayer of charged gold nanocrystals at the water/oil interface, Angew. Chem. Int. Ed. 43

(2004), 458–462.

[59] Y.-K. Park, S.-H. Yoo, S. Park, Assembly of highly ordered nanoparticle monolayers at a water/hexane interface, Langmuir, 23 (2007), 10505–10510.

[60] V. Aleksandrovic, D. Greshnykh, I. Randjelovic, A. Frömsdorf, A. Kornowski, S. V. Roth, C. Klinke, H. Weller, Preparation and electrical properties of cobalt−platinum nanoparticle monolayers deposited by the langmuir−blodgett technique, ACS Nano 2 (2008), 1123–1130.

[61] T. Ishida, T. Tatsuma, Effect of plasmon coupling on quantum efficiencies of plasmon-induced charge separation, J. Phys. Chem. C 122 (2018), 26153–26159.

[62] P. Pallavicini, L. De Vita, F. Merlin, C. Milanese, M. Borzenkov, A. Taglietti, G. Chirico, Suitable polymeric coatings to avoid localized surface plasmon resonance hybridization in printed patterns of photothermally responsive gold nanoinks, Molecules 2020, 25, 2499.

[63] A. J. Bovill, A. A. McConnell, J. A. Nimmo, W. E. Smith, Resonance Raman spectra of .alpha.-copper phthalocyanine, J. Phys. Chem. 90 (1986), 569–575.